ELSEVIER

Thermochimica Acta 366 (2001) 135–147

thermochimica acta

www.elsevier.com/locate/tca

Calorimetric evaluation of phase change materials for use as thermal interface materials

Zongrong Liu, D.D.L. Chung*

Composite Materials Research Laboratory, State University of New York at Buffalo, Buffalo, NY 14260-4400, USA

Received 16 May 2000; received in revised form 17 August 2000; accepted 26 August 2000

Abstract

The phase change behavior of organic and inorganic phase change materials, namely paraffin wax, microcrystalline wax, $Na_2SO_4 \cdot 10H_2O$ and $CaCl_2 \cdot 6H_2O$, with melting temperatures close to room temperature, was evaluated by differential scanning calorimetry. The melting and solidification temperatures, supercooling, heat of fusion and thermal cycling stability of these materials, with and without additives, were determined. Paraffin wax, with or without α-Al_2O_3 or BN particles, are potentially good thermal interface materials, because of the negative supercooling (down to $-7^{\circ}C$), large heat of fusion (up to 142 J/g) and excellent thermal cycling stability. Microcrystalline wax is not suitable, due to its unclear endothermic and exothermic peaks and wide melting temperature range. The addition of 20–60 wt.% α-Al_2O_3 to paraffin wax decreases the melting temperature by $7^{\circ}C$. Beyond 60 wt.% α-Al_2O_3, the melting temperature of paraffin wax increases toward the value without α-Al_2O_3. The heat of fusion of paraffin wax attains a minimum at 20 wt.% α-Al_2O_3. The addition of BN has little effect on the phase change behavior of paraffin wax. The inorganic materials $Na_2SO_4 \cdot 10H_2O$ and $CaCl_2 \cdot 6H_2O$, with and without nucleating additives, are not suitable for use as thermal interface materials, due to the incongruent melting and decomposition behavior, large supercooling ($8^{\circ}C$ or more) and thermal cycling instability.

Keywords: Phase change; Calorimetry; Wax; Sodium sulfate; Calcium chloride; Aluminum oxide; Boron nitride; Thermal interface

1. Introduction

Due to the miniaturization and increased power of electronics, much heat is generated during their operation. Much research work has been done to dissipate the heat generated by electronic components during use to reduce the adverse effects of heat on the performance of the electronics. Heat transfer is also encountered in heat exchangers, deicing and numerous industrial processes. A common method of heat dissipation is to use heat sinks [1–3]. Different materials such as metals (e.g. silver, copper and aluminum) [1], diamond [2] and composites [3] are effective heat sink materials because of their high thermal conductivity. In order to obtain effective heat dissipation, a low thermal resistance of the interface between the heat sink and the heat source is also crucial. The effectiveness of heat dissipation depends in part on the geometric cross-sectional area of the conductive path and in part on the degree of smoothness of the adjoining surfaces of the device and of the heat sink. However, the surfaces usually are not perfectly

* Corresponding author. Tel.: +1-716-645-2593; fax: +1-716-645-3875.
E-mail address: ddchung@acsu.buffalo.edu (D.D.L. Chung).

0040-6031/01/$ – see front matter
PII: S0040-6031(00)00716-4

smooth. Irregularities on the surfaces of heat sink and heat source, even in a microscopic scale, form pockets and gaps in which air can be entrapped. These pockets and gaps reduce the efficiency of the heat transfer because of the reduced effective area and the low thermal conductivity of air (0.027 W/m °C). To alleviate these problems, a thermal interface material [4–12] is used between the heat sink and the heat source to fill in the surface irregularities and eliminate the air pockets and gaps. Due to the small size of current electronic components and the relatively low thermal conductivity of the thermal interface materials, a thermal interface material needs to be applied in the form of a film. Desired properties of thermal interface materials include high thermal conductivity, high fluidity (consequently high conformability to the surfaces of heat sink and heat source) and good thermal stability.

The total thermal resistance through a thermal interface includes the thermal resistance of the interface between the thermal interface material and the heat sink, the thermal resistance of the interface between the thermal interface material and the heat source, and the thermal resistance of the thermal interface material itself. Most research work was focused on application development of various thermal interface materials, among which are some polymers with relatively high thermal conductivity, such as urethane [11], polyimide [13] and polytetrafluoroethylene [14]. However, they usually need pressure to be applied on the contact, because of the low fluidity and conformability.

A liquid or semi-liquid usually has good fluidity, and therefore, high conformability. Pastes based on a liquid or semi-liquid carrier and containing powders of high thermal conductivity for use as thermal interface materials are described in numerous patents [6,10,15]. The most common carrier is silicone [16]. The disadvantages of silicone grease are messiness and difficulty of removal by dissolution. Silicone rubber was tried as a carrier to replace silicone grease. However, it needs higher pressure and sometimes, even under pressure it still does not fill the air gaps, due to its higher viscosity and consequent less conformability. A common disadvantage of using a liquid or semi-liquid carrier is that it tends to flow out, whether it is in service or not. Thus, a better choice is a carrier which is in the solid state at room temperature and in the liquid or semi-liquid state at the higher service temperature. Hence, a phase change material (PCM), which changes to the liquid state from the solid state while it is in service, is potentially attractive for use as a thermal interface material.

The PCMs, usually meaning solid–liquid phase change materials (because the latent heat change for a solid-to-solid transition is usually considerably less than that for a solid-to-liquid transition), have received considerable attention in recent years due to their high heat storage capacity [17–22]. Various forms of PCMs have been utilized as thermal storage media for cooling and heating applications [23–25]. A difference between previous work and the present work on PCMs is that most PCMs tested previously were tested in the encapsulated state in order to avoid the gain or loss of moisture (especially in the case of salt hydrate materials), and vaporization (especially in the case of organic PCMs). PCMs, especially the organic compounds in the present work, were kept in a nearly open system during calorimetric testing, as thermal interface materials are sometimes not used in a completely closed system.

The PCMs can be roughly classified as inorganic compounds (mainly salt hydrates) [22] and organic compounds [25–27], although inorganic ones are much more common. A review of PCMs for use as latent heat materials was given by Lane [17]. Abhat [28] also reviewed a number of materials with low melting temperatures (0–120°C).

Organic PCMs can be classified as paraffins and non-paraffin organics. A detailed discussion of the properties of paraffins can be found in [29]. Himran et al. [30] reviewed paraffin waxes for use as energy storage materials. Due to their high latent heat, PCMs as a possible thermal management solution for commercial electronic products have received increasing attention in recent years [31–33]. Pal and Joshi [31] studied the thermal control of a heat source by using a paraffin, *n*-triacontane, housed in a sealed heat sink close to the heat source. Numerical analysis of a finned surface surrounded by a paraffin (nonadecane) was studied for high heat flux levels [32]. However, at high heat flux levels, the poor thermal conductivity of PCMs limits their thermal control performance.

$Na_2SO_4 \cdot 10H_2O$ and $CaCl_2 \cdot 6H_2O$, with their melting temperature (about 30°C) slightly above room

temperature, are two typical inorganic PCMs. Telks [34] used $Na_2SO_4 \cdot 10H_2O$ to build the first PCM-heated solar house shortly after the end of the second World War. $CaCl_2 \cdot 6H_2O$ was investigated for passive applications, as in heat pumps, and in forced air heating systems in the 1970s [17]. $CaCl_2 \cdot 6H_2O$ was mentioned as a thermal energy storage material [22].

Common problems associated with inorganic PCMs are supercooling and thermal instability. Since solidification involves nucleation, numerous nucleating additives have been investigated in order to reduce the supercooling. Although a nucleator with a crystal structure similar to the PCM and with little solubility in the PCM is preferred, many nucleators were found just by intuition with no explanation of their effectiveness. Telks [34] tested several isostructural nucleation additives and found that $Na_2B_4O_7 \cdot 10H_2O$ was the best nucleator for $Na_2SO_4 \cdot 10H_2O$, which reduced the supercooling of $Na_2SO_4 \cdot 10H_2O$ (about 15°C) to the range of 1.4–1.9°C. The nucleation of $CaCl_2 \cdot 6H_2O$ was studied by numerous workers. $BaI_2 \cdot 6\ H_2O$ [35], BaO and $Ba(OH)_2$ [17], copper powder [36], Al_2O_3 [37], $NiCl_2 \cdot 6H_2O$ [38] and many other additives were found to help the nucleating of $CaCl_2 \cdot 6H_2O$.

The reliability of PCMs is much better than that of thermal pastes based on liquid and semi-liquid carriers. In addition, the performance may be enhanced by mixing the PCM with polymers and with particulate fillers of high thermal conductivity. However, most PCMs with high energy storage density have an unacceptably low thermal conductivity. Generally speaking, a PCM with melting temperature a little above room temperature, large heat of fusion, low viscosity in the liquid state, small or negative supercooling (defined in Section 2), good thermal cycling stability and thermal conductivity is attractive for use as a thermal interface material.

In this work, the evaluation of PCMs for use as thermal interface materials is limited to a calorimetric investigation of the heat of fusion, melting temperature, stability to thermal cycling and supercooling. The effects of thermally conductive particulate fillers and nucleating additives to PCMs are also addressed. The objective of this paper is to study the phase change behavior of organic and inorganic PCMs for use as thermal interface materials in electronics. The evaluation of the actual performance as thermal interface materials is the subject of a separate publication.

2. Experimental methods

2.1. Materials

The organic compound PCMs were paraffin and microcrystalline waxes. The additives to the organic PCMs were hexagonal Al_2O_3 platelets and hexagonal BN, which have attractive thermal conductivity. The inorganic compound PCMs tested included sodium sulfate decahydrate and calcium chloride hexahydrate. The additives used to modify the phase change behavior of the inorganic PCMs were potassium bromide, calcium bromide hydrate, borax decahydrate, copper powder, BaO, $NiCl_2 \cdot 6H_2O$, $Ba(OH)_2$ and $Ba(OH)_2 \cdot 8H_2O$.

The paraffin wax, predominantly tricosane paraffin ($C_{23}H_{48}$), was supplied by Crystal, Inc.-PMC, Lansdale, PA. The microcrystalline wax, a mixture of paraffins (C_nH_{2n+2}, $19 \leq n \leq 25$) derived from petroleum and characterized by the fineness of its crystals (in contrast to the larger crystals of paraffin wax), was supplied by Strahl & Pitsch Inc., West Babylon, NY.

Borax (sodium tetraborate) decahydrate ($Na_2B_4O_7 \cdot 10H_2O$) was obtained from Sigma Chemical Co., St. Louis, MO. The sodium sulfate decahydrate powder ($Na_2SO_4 \cdot 10H_2O$, >99.0%) was purchased from EM Science, Gibbstown, NJ. The calcium chloride hexahydrate ($CaCl_2 \cdot 6H_2O$, >98.0%), barium hydroxide ($Ba(OH)_2$, >95%), barium hydroxide octahydrate ($Ba(OH)_2 \cdot 8H_2O$, 98%) was purchased from Aldrich Chemical Company Inc., Milwaukee, WI. The barium oxide (BaO, >90.0%) granules were also from Aldrich Chemical Company Inc., with a size of 20 mesh. This powder had been ground to a size finer than −450 mesh before being used in the present work. Nickel chloride hexahydrate ($NiCl_2 \cdot 6H_2O$, >97%) was purchased from Fisher Scientific Co., Fair Lawn, NJ. Hexagonal α-Al_2O_3 platelets (>98.14%), with an average size of 3.2 μm, was from Micro Abrasives Corp., Westfield, MA. Hexagonal boron nitride (BN) particles were from Advanced Ceramics Corp., Cleveland, OH. Their size was about 5–11 μm. Copper powder (>99%), with a size of about 1 μm, was supplied by Ultrafine Powder Technology Inc., Woonsocket, RI.

2.2. Composition preparation

Each composition consisting of PCM and additives was prepared by manual mixing of the components for 15 min at a temperature slightly higher than the melting point of the PCM. Organic PCMs (paraffin wax and microcrystalline wax) were tested using differential scanning calorimetry (DSC). The effect of microcrystalline wax on the thermal behavior of paraffin wax was examined by testing mixtures of paraffin wax with 90, 80, 60, 40, 20 and 10 wt.% microcrystalline wax (corresponding, respectively, to 89.8, 79.6, 59.3, 39.3, 19.6 and 9.8 vol.% microcrystalline wax). DSC was also carried out on paraffin wax with 90, 80, 60, 40, 20 and 10 wt.% α-Al_2O_3 (corresponding, respectively, to 65.7, 50.0, 24.2, 12.4, 5.1 and 2.3 vol.% α-Al_2O_3), and on paraffin wax with 20 wt.% BN (corresponding to 8.6 vol.% BN), in order to study the effect of inorganic compounds on the thermal behavior.

Three compositions involving sodium sulfate decahydrate were chosen for DSC analysis, namely (1) pure sodium sulfate decahydrate; (2) sodium sulfate decahydrate with 1–5 wt.% (corresponding to 0.8–4.2 vol.%) borax decahydrate; and (3) 80 wt.% (sodium sulfate decahydrate with 1–5 wt.% borax decahydrate) plus 20 wt.% α-Al_2O_3 (corresponding 0.8–3.8 vol.% $Na_2B_4O_7{\cdot}10H_2O$, 87.6–90.6% $Na_2SO_4{\cdot}10H_2O$ and 8.6 vol.% Al_2O_3).

Calcium chloride hexahydrate with and without additives (<5 wt.%, namely BaO, KBr, Cu, $NiCl_2{\cdot}6H_2O$, $Ba(OH)_2$ and $Ba(OH)_2{\cdot}8H_2O$), were tested using DSC.

2.3. Setting of the thermal cycle temperature range

In order to estimate the melting and solidification temperatures of the organic and inorganic compounds for the purpose of selecting the thermal cycle temperature range, each compound was sealed in a small transparent glass bottle and then put in a water bath. Melting and solidification of a compound were visually observed by manually shaking the bottle in the water bath and by measuring the temperature of the water during heating or cooling. The lowest temperature in the thermal cycling in the present work was 10°C, because of the difficulty of using PCMs with solidification temperatures below room temperature as thermal interface materials. The thermal cycle temperature in this work ranged from 10 to 90°C.

2.4. Calorimetric analysis

All inorganic samples were sealed in aluminum pans and all organic compounds were just put in aluminum pans and covered by aluminum lids. Then all samples were tested in air by DSC, using a Perkin-Elmer Corp. (Norwalk, CT) DSC 7 system equipped with an Intracooler. The heating and cooling rates were 2.0°C/min.

The phase change onset temperature (T_s) [39] corresponds to the point of intersection of the tangent (drawn at the point of maximum slope of the leading edge of the DSC peak) and the extrapolated baseline on the same side as the leading edge of the peak. The temperature corresponding to the DSC peak is referred to as T_p. Since the x-axis displays the temperature, the onset temperature is on the left side of a DSC peak during heating and on the right side of a peak during cooling. The melting and solidification points mentioned in the following sections are both T_s. The T_s and heat of fusion (ΔH) were calculated by using programs provided by Perkin-Elmer Corp. for this purpose. The supercooling (ΔT) here is the temperature difference between T_s during heating and T_s during cooling for the same thermal cycle. The supercooling is positive if T_s during heating is higher than that during cooling, and is negative if T_s during heating is lower than that during cooling.

3. Results and discussion

3.1. Organic PCMs

Fig. 1 shows the DSC curves of paraffin wax. Thirty thermal cycles were conducted. The T_s, T_p, ΔT and ΔH for the first, second and 30th cycle are listed in Table 1. They almost had the same values for the 30th cycle as the second cycle, indicating good stability of thermal cycling. The difference between the first cycle and subsequent cycles may be caused by the contact between the sample and the aluminum pan improving after the first cycle due to the melting of paraffin wax in the first cycle. The supercooling was quite independent of the cycle number and was negative. The T_s

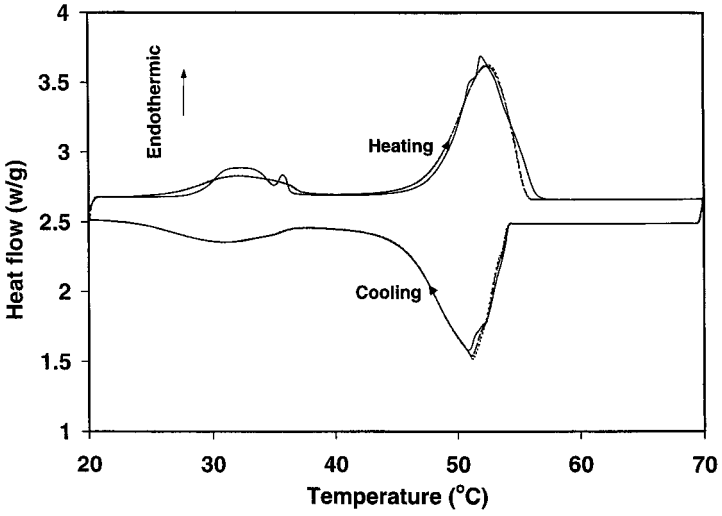

Fig. 1. DSC curves of paraffin wax: (—) first cycle; (– – –) second cycle; (- - -) third cycle.

during cooling was above room temperature. This means that the PCM is in the solid state when it is not in service. The heat of fusion was also very large. Thus, paraffin wax is suitable for use as a thermal interface material.

Fig. 2 is the DSC curves of microcrystalline wax. Three thermal cycles were conducted. Unlike the paraffin wax, it had no clear exothermic or endothermic peak. The phase change occurred over a range of temperatures. It is difficult to use this kind of wax as a thermal interface material, because it has low fluidity, and thus, poor conformability. For many organic PCMs, the change of phase takes place over a temperature range, thus resulting in a mushy zone in which solid and liquid phases coexist [40]. The solid part may have an adverse effect on the performance of the PCM because only the liquid part is desired for conformability. Thus, if this PCM is used as a thermal interface material, it should have good thermal conductivity.

Fig. 3 is typical DSC curves of a composite of paraffin and microcrystalline waxes (80 wt.%). Two thermal cycles were conducted. These curves have a composite feature of the two wax types. The mixtures with 90, 60, 40, 20 and 10 wt.% microcrystalline wax were also tested. It was found that the mixture had a shape of DSC curves close to that of microcrystalline wax if microcrystalline wax was dominant, and the shape was close to that of paraffin wax if paraffin wax in the mixture was dominant.

Paraffin wax tested here had sharper endothermic and exothermic peaks because its main composition was tricosane, with its melting temperature about 47.7°C. The different thermal behavior of microcrystalline wax compared to paraffin wax is caused by the mixed composition of microcrystalline wax. The

Table 1
DSC data for the dominant peak for paraffin wax during different thermal cycles

Cycle number	1		2		30	
	Heating	Cooling	Heating	Cooling	Heating	Cooling
T_s (°C)	48.9	54.2	47.7	53.8	47.7	53.8
T_p (°C)	52.0	50.9	52.5	51.1	52.5	51.2
ΔT (°C)	−5.3	−5.3	−6.1	−6.1	−6.1	−6.1
ΔH (J/g)	142.3	−143.9	142.6	−145.6	140.1	−144.6

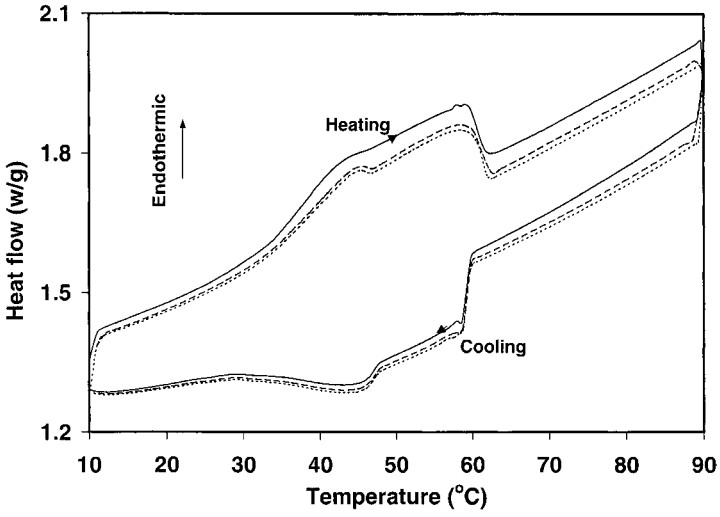

Fig. 2. DSC curves of microcrystalline wax: (—) first cycle; (– – –) second cycle; (- - -) third cycle.

melting temperatures of nonadecane ($C_{19}H_{40}$), eicosane ($C_{20}H_{42}$), heneicosane ($C_{21}H_{44}$), docosane ($C_{22}H_{46}$), tricosane ($C_{23}H_{48}$), tetracosane ($C_{24}H_{50}$) and pentacosane ($C_{25}H_{52}$) in the mixed composition of microcrystalline wax are 31.4, 36.7, 40.4, 45.7, 47.7, 49.4 and 53.3, respectively [29]. A mixture of two or more of these paraffins is associated with a range of melting temperatures.

The effect of inorganic compounds on paraffin wax was also investigated. The inorganic compounds used here were α-Al_2O_3 and BN, which have high thermal conductivity compared to the wax and are electrical insulators. Fig. 4 is typical DSC curves of the mixture of 80 wt.% paraffin wax and 20 wt.% Al_2O_3. Thirty thermal cycles were conducted. The T_s, T_p, ΔT and ΔH for the first, second and 30th cycle are listed in Table 2. The stability of the mixture to thermal cycling is clear. Compared to the DSC data of the paraffin wax shown in Table 1, the heat of fusion decreased significantly, as also shown in Fig. 5, where the calculated (based on

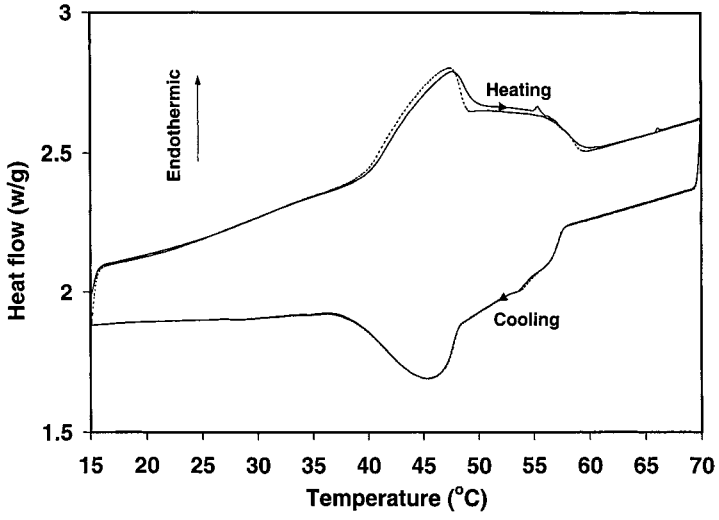

Fig. 3. Typical DSC curves of a composite of paraffin wax with 80 wt.% microcrystalline wax: (—) first cycle; (- - -) second cycle.

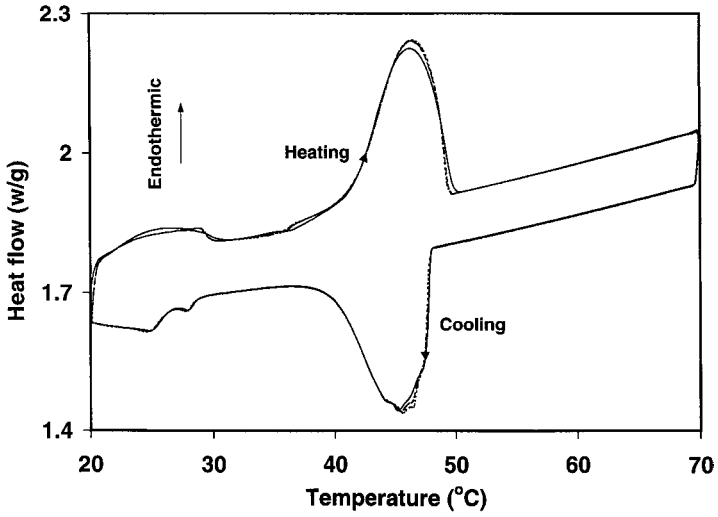

Fig. 4. Typical DSC curves of a composite of paraffin wax with 20 wt.% α-Al_2O_3 particles: (—) first cycle; (– – –) second cycle; (- - -) third cycle.

the Rule of Mixtures) and experimental values of ΔH are shown. The melting point of the mixture decreased by about 7°C. That the melting point during heating was closer to room temperature is helpful for using this kind of PCM as a thermal interface material, because it will result in a decrease in the temperature at which the PCM will be in the liquid state. In addition, the negative supercooling is helpful, because the PCM will solidify at a higher temperature when the system is cooling and this will reduce the further flowing out of the PCM when the system is not in use.

The mixtures with 90, 80, 60, 40, and 10 wt.% α-Al_2O_3 were also tested. The calculated heat of fusion (corresponding to the solid circles in Fig. 5) decreased linearly with increasing proportion of Al_2O_3. The measured ΔH decreased sharply when the proportion of Al_2O_3 exceeded 10 wt.%. A minimum in the measured ΔH was observed at 20 wt.% Al_2O_3. The effect of α-Al_2O_3 on the melting temperature of paraffin wax is shown in Fig. 6. Figs. 5 and 6 correspond to the second thermal cycle during heating. The melting points of the mixtures decreased by 7°C when the content of α-Al_2O_3 was in the range of 20–60 wt.%. Further addition of α-Al_2O_3 to paraffin wax resulted in an increase in the melting temperature, which reached 47.2°C (close to the melting point of pure paraffin wax, 47.7°C) when the proportion of α-Al_2O_3 exceeded 80 wt.%.

The effect of adding 20 wt.% BN to paraffin wax is shown in Fig. 7. Thirty thermal cycles were conducted. The T_s, T_p, ΔT and ΔH for the first, second and 30th cycle are listed in Table 3. The mixture also exhibited good stability to thermal cycling. ΔH was 113.3 J/g for the second cycle during heating. Based on the DSC data of the paraffin wax shown in Table 1 and the calculated curve in Fig. 5, the calculated heat

Table 2
DSC data for the dominant peak for paraffin wax with 20 wt.% $A1_2O_3$ during different thermal cycles

Cycle number	1		2		30	
	Heating	Cooling	Heating	Cooling	Heating	Cooling
T_s (°C)	41.0	48.0	41.0	48.0	41.0	47.9
T_p (°C)	46.2	45.2	46.2	45.5	46.4	45.6
ΔT (°C)	−7.0	−7.0	−7.0	−7.0	−6.9	−6.9
ΔH (J/g)	57.9	−58.0	59.8	−58.8	59.8	−56.3

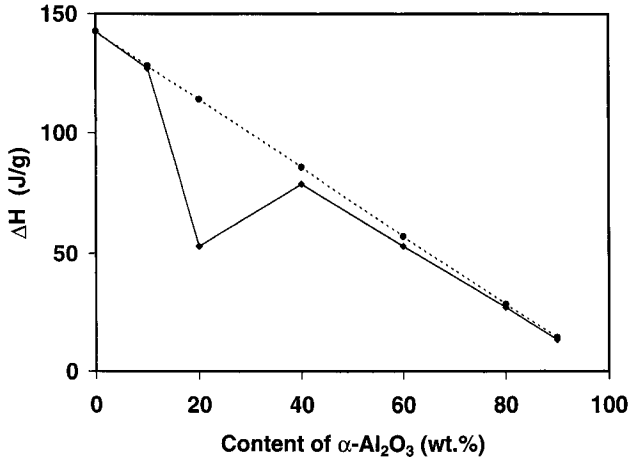

Fig. 5. The effect of α-Al_2O_3 particles on the heat of fusion of paraffin wax: (—) experimental curve; (– – –) calculated curve.

of fusion of paraffin wax with 20 wt.% BN is 114.1 J/g. This indicates that the addition of BN to paraffin wax did not change the heat of fusion of paraffin wax. Comparison of Tables 1 and 3 shows that the addition of BN to paraffin wax did not affect T_s or T_p.

Both Al_2O_3 and BN had good thermal conductivity. However, their addition to paraffin wax resulted in different effects on T_s, ΔT and ΔH, as mentioned above. The lower T_s and ΔH of paraffin wax due to the addition of 20 wt.% Al_2O_3 suggest that Al_2O_3 caused the wax molecules to move more easily during heating, probably due to the adsorption of the wax molecules in the liquid state on the fine Al_2O_3 particles. The liquid wax, due to local melting, spread on the surface of Al_2O_3 particles, and thus, increased the contact area between the liquid wax and the solid part of the wax. This would facilitate the movement and diffusion of the molecules of the solid wax into the liquid part. Thus, increasing the content of Al_2O_3 particles to 20 wt.% decreased the melting temperature of paraffin wax. On the other hand, the Al_2O_3 particles were also barriers to the diffusion and movement of liquid wax. Consequently, further addition of Al_2O_3 particles (beyond 60 wt.%) resulted in an increase of the melting temperature of paraffin wax. The effect of different kinds of inorganic compounds

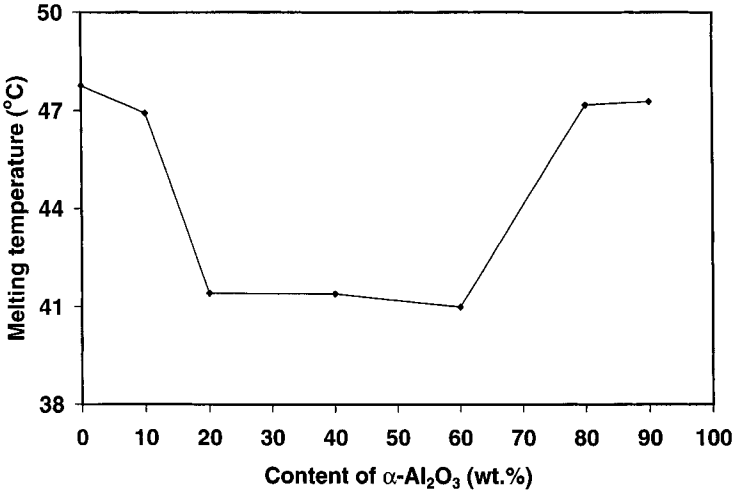

Fig. 6. The effect of α-Al_2O_3 on the melting temperature of paraffin wax.

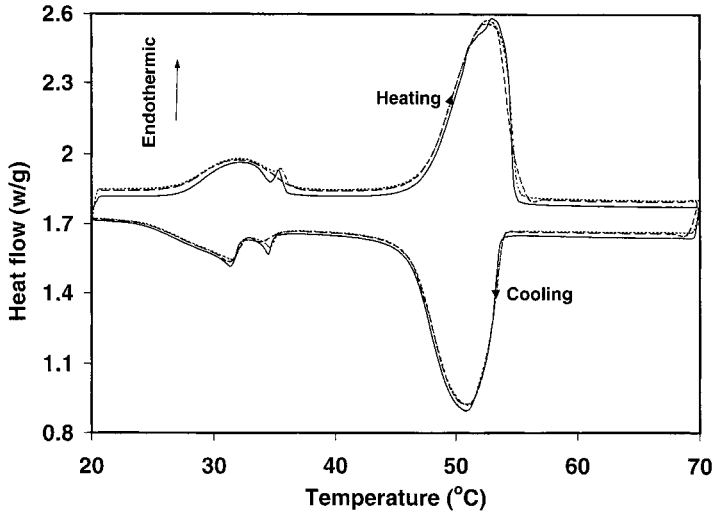

Fig. 7. Typical DSC curves of a composite of paraffin wax with 20 wt.% BN particles: (—) first cycle; (– – –) second cycle; (- - -) third cycle.

on the thermal behavior of paraffin wax needs further study.

3.2. Inorganic PCMs

Fig. 8(a) shows the DSC curve of $Na_2SO_4{\cdot}10H_2O$. Its melting temperature (T_s) during heating is about 28.2°C. ΔH is 102.1 J/g. An exothermic peak was not observed during cooling from 60 to 10°C. A part of $Na_2SO_4{\cdot}10H_2O$ began to solidify at 48.5°C upon cooling while the solidification of the rest occurred at less than 10°C (not shown in Fig. 8(a)). The supercooling (ΔT) of the latter part was more than 18°C.

Fig. 8(b) is typical DSC curves of $Na_2SO_4{\cdot}10H_2O$ with 1 wt.% $Na_2B_4O_7{\cdot}H_2O$. Three cycles were conducted. An endothermic peak (during heating) and an exothermic peak (during cooling) were observed in each of the first two cycles, but an exothermic peak was hardly observed in the third cycle. The T_s, T_p, ΔT and ΔH of the three cycles are listed in Table 4. The T_s during heating decreased slightly with increasing thermal cycle number. The supercooling (ΔT) was more than 8°C. The latent heat of fusion decreased significantly with increasing cycle number. ΔH was almost zero during cooling in the third thermal cycle.

The supercooling clearly decreased upon the addition of $Na_2B_4O_7{\cdot}10H_2O$ to $Na_2SO_4{\cdot}10H_2O$ under the condition used in the present work. However, it was not as small as that described by Telks [34], which was less than 2°C. We also investigated the effect of the addition of Al_2O_3 on the mixture of $Na_2SO_4{\cdot}10H_2O$ and $Na_2B_4O_7{\cdot}10H_2O$. The resultant reduction in supercooling was very small. The decrease in ΔH with increasing cycle number may be due to the decomposition [17] and incongruent melting behavior of $Na_2SO_4{\cdot}10H_2O$. The incongruent melting behavior

Table 3
DSC data for the dominant peak for paraffin wax with 20 wt.% BN during different thermal cycles

Cycle number	1		2		30	
	Heating	Cooling	Heating	Cooling	Heating	Cooling
T_s (°C)	48.5	53.6	47.4	53.8	47.4	53.9
T_p (°C)	53.0	50.8	52.7	50.9	52.7	50.9
ΔT (°C)	−5.1	−5.1	−6.4	−6.4	−6.5	−6.5
ΔH (J/g)	112.3	−116.2	113.3	−115.5	112.7	−117.0

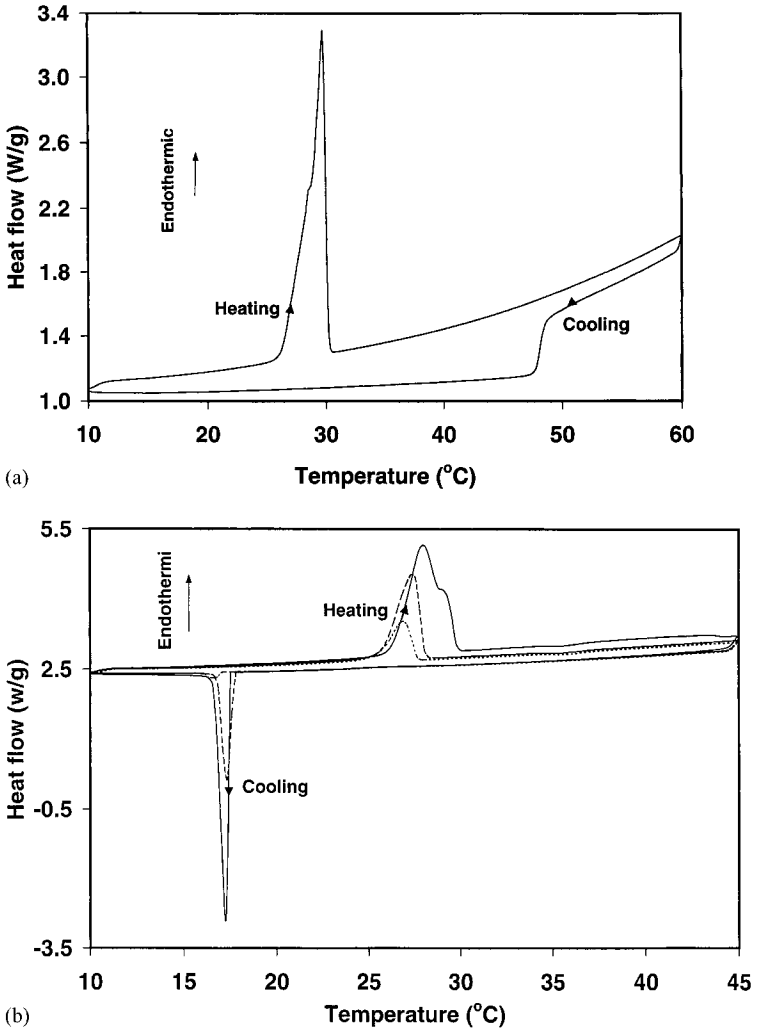

Fig. 8. DSC curves of $Na_2SO_4{\cdot}10H_2O$ (a) without additives and (b) with 1 wt.% $Na_2B_4O_7{\cdot}10H_2O$: (—) first cycle; (– – –) second cycle; (- - -) third cycle.

Table 4
DSC data for inorganic PCM consisting of 99 wt.% $Na_2SO_4{\cdot}10H_2O$ and 1 wt.% $Na_2B_4O_7{\cdot}H_2O$ during the first three thermal cycles

Cycle number	1		2		3	
	Heating	Cooling	Heating	Cooling	Heating	Cooling
T_s (°C)	26.4	17.5	25.8	17.8	25.4	17.2
T_p (°C)	28.0	17.2	27.4	17.3	26.9	16.6
ΔT (°C)	8.9	8.9	8.0	8.0	8.2	8.2
ΔH (J/g)	97.3	−48.2	52.3	−26.1	23.3	−1.5

was observed in the experiment to set the thermal cycle temperature range, as mentioned in Section 2. It was found in this experiment that a part of $Na_2SO_4{\cdot}10H_2O$ would not melt during heating and most of it became solid after several thermal cycles. It is difficult to use $Na_2SO_4{\cdot}10H_2O$ as a thermal interface material because of its decomposition behavior, large supercooling and incongruent melting behavior. Actually, Telk's PCM-heated house failed in the third winter due to the separation of $Na_2SO_4{\cdot}10H_2O$ into anhydrous and supernatant layers and the loss of the heat storage capacity, although the material was tightly sealed in cans.

Fig. 9(a) is the DSC curve of $CaCl_2{\cdot}6H_2O$. No exothermic peak was observed during cooling from 60 to 10°C. The T_s, T_p and ΔH were 19.9 and 25°C, and 150.5 J/g, respectively, during heating. Fig. 9(b) shows typical DSC curves of $CaCl_2{\cdot}6H_2O$ containing 1 wt.% BaO. Three cycles were conducted. Endothermic and exothermic peaks were observed during heating and cooling, respectively. Table 5 shows the DSC data for this composition during the first three thermal cycles. The T_s remained nearly constant during heating with increasing thermal cycle number. However, T_s during cooling decreased in the second cycle but increased in the third cycle. Two exothermic

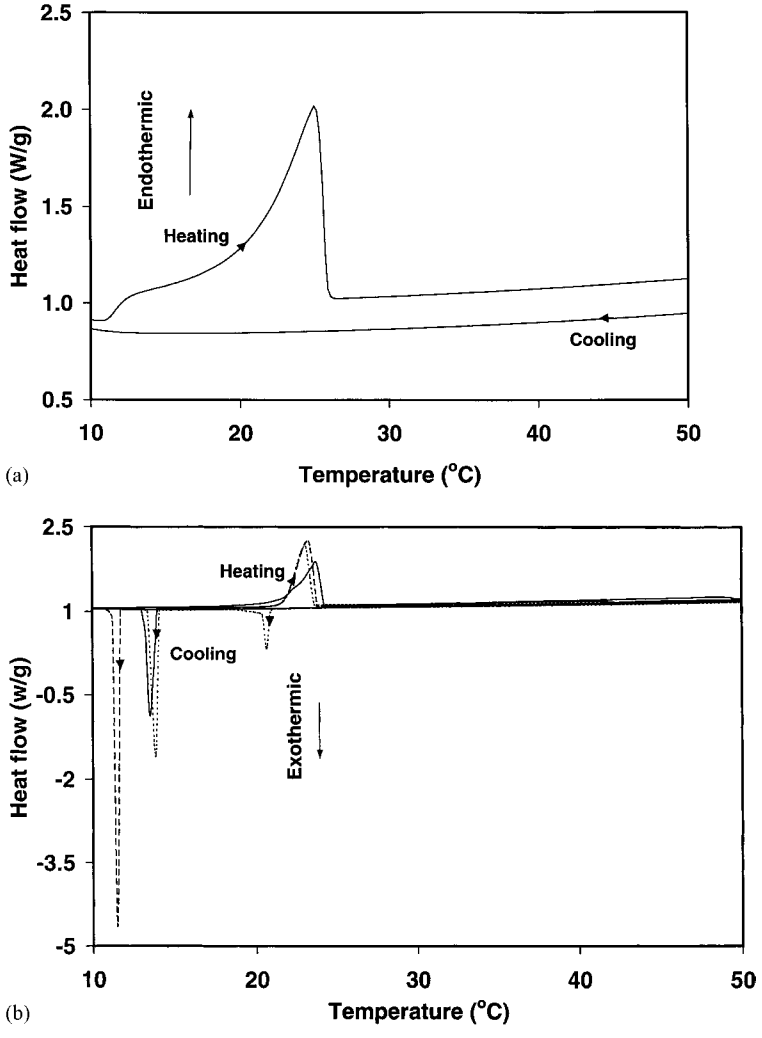

Fig. 9. DSC curves of $CaCl_2{\cdot}6H_2O$ (a) without additives and (b) with 1 wt.% BaO: (—) first cycle; (– – –) second cycle; (- - -) third cycle.

Table 5
DSC data for inorganic PCM consisting of 99 wt.%$CaCl_2 \cdot 6H_2O$ and 1 wt.% BaO during the first three thermal cycles[a]

Cycle number	1		2		3	
	Heating	Cooling	Heating	Cooling	Heating	Cooling
T_s (°C)	21.9	14.0	21.8	11.7	21.8	13.9(20.8)
T_p (°C)	23.7	13.5	23.2	11.5	23.0	13.8 (20.7)
ΔT (°C)	7.9	7.9	10.1	10.1	7.9 (1.0)	7.9 (1.0)
ΔH (J/g)	142.7	−105.8	163.9	−118.9	135.1	−131.9 (−26.2)

[a] The values in parentheses correspond to the smaller exothermic peak during cooling in the third cycle.

peaks were observed in the third cycle during cooling. Exothermic peaks were seldom observed after three thermal cycles. With the addition of BaO, the supercooling was reduced to about 8°C. The complex thermal behavior was caused by the interaction of the nucleating ability of BaO and the absorption of moisture by $CaCl_2 \cdot 6H_2O$. The addition of BaO made the nucleation of $CaCl_2 \cdot 6H_2O$ easier and reduced the supercooling during the first several thermal cycles. However, the absorption of moisture by $CaCl_2 \cdot 6H_2O$ made the nucleation more difficult, due to the high solubility of $CaCl_2 \cdot 6H_2O$ in water. This resulted in the absence of exothermic peaks after several thermal cycles.

Other additives such as $NiCl_2 \cdot 6H_2O$, Cu, $Ba(OH)_2$ and $Ba(OH)_2 \cdot 8H_2O$ had similar effects on the DSC behavior of $CaCl_2 \cdot 6H_2O$ as BaO. The common phenomena were that (1) the exothermic peak during cooling disappeared at a certain thermal cycle, i.e. it disappeared in the second or third thermal cycle, or no exothermic peak was observed even in the first cycle and (2) double peaks occurred during cooling or heating. The endothermic and exothermic peaks for $CaCl_2 \cdot 6H_2O$ with and without additives were very complex.

It is difficulty to use inorganic PCMs as thermal interface materials. Unlike organic PCMs, inorganic PCMs have large supercooling and poor thermal cycling stability. The heat of fusion for inorganic compounds usually is large, especially for $CaCl_2 \cdot 6H_2O$. However, the idea to develop thermal interface materials from PCMs is based on their good fluidity in the molten state, although a large heat of fusion during heating is preferred for the purpose of heat absorption. In addition, the corrosion of container [17] due to the inorganic PCMs may also limit the use of inorganic PCMs as thermal interface materials.

4. Conclusions

1. Paraffin wax has clear endothermic and exothermic DSC peaks, excellent thermal cycling stability, large heat of fusion (up to 142 J/g) and negative supercooling (down to −7°C), and thus, is a good candidate for use as a thermal interface material. Mixtures of paraffin wax and inorganic additives (α-Al_2O_3 and BN) are also attractive.
2. The addition of α-Al_2O_3 (20–60 wt.%) to paraffin wax decreases the melting temperature by 7°C. Upon increasing the proportion of α-Al_2O_3 beyond 60 wt.%, the melting temperature increases toward the value for the case without α-Al_2O_3. The heat of fusion attains a minimum at 20 wt.% α-Al_2O_3.
3. BN has no significant effect on the phase change behavior of paraffin wax.
4. The organic PCM microcrystalline wax has no clear endothermic or exothermic DSC peak and has a wide melting temperature range. It has low fluidity and poor conformability in the melting temperature range. Thus, it is not suitable for use as a thermal interface material. The phase change behavior of mixtures of microcrystalline wax and paraffin wax has characteristics of both waxes.
5. Inorganic PCM $Na_2SO_4 \cdot 10H_2O$, with and without nucleator $Na_2B_4O_7 \cdot 10H_2O$, has poor thermal cycling stability and incongruent melting behavior, although the addition of the nucleator reduces the supercooling of $Na_2SO_4 \cdot 10H_2O$ to about 8°C (still large). These inorganic materials are not suitable for use as thermal interface materials.
6. Inorganic PCM $CaCl_2 \cdot 6H_2O$, with or without additives such as BaO, $NiCl_2 \cdot 6H_2O$, Cu, $Ba(OH)_2$ and $Ba(OH)_2 \cdot 8H_2O$, has poor thermal cycling

stability and is not suitable for use as a thermal interface material.

Acknowledgements

This work was supported in part by Defense Advanced Research Projects Agency, USA.

References

[1] Y. Nakamura, M. Kawakami, Heat-Conductive Material and Method of Producing the Same, US Patent 5,358,795 (1994).
[2] M. Simpson, Thermal Management of Electronic Components Using Synthetic Diamond, EP 00661740A2 (1995).
[3] Y. Nakamura, K. Hirano, Method of Preparing a Heat-Conductive Composite Material, EP 432867 (1996).
[4] C.A. Latham, M.F. McGuiggan, Thermally Conductive Ceramic/Polymer Composites, US Patent 5,011,872 (1991).
[5] M.H. Bunyan, Double-side Thermally Conductive Adhesive Tape for Plastic-Packaged Electronic Components, WO 9905722 (1999).
[6] M. Toya, Thermal Conductive Silicone Composition, US Patent 5,021,494 (1991).
[7] J. Ziemski, P. Khatri, Sprayable Thermal Grease, EP 0906945 (1999).
[8] M. Welxel, Thermal Interface Pad Assembly, EP 00875933 (1998).
[9] J. Block, R.W. Rice, C.R. Morgan, Thermally Conductive Elastomer, US Patent 5,194,480 (1993).
[10] K.L. Hanson, Semisolid Thermal Interface with Low Flow Resistance, EP 0813244 (1997).
[11] V. Squitieri, Thermally Conductive Materials, US Patent 4,869,954 (1989).
[12] C.D. Lacovangelo, P.J. Diconza, Thermally Conductive Material, EP 696063 (1996).
[13] D.C. DeGree, H.J. Fick, B.H. Juenger, Thermally Conductive, Electrically Insulative Laminate, US Patent 4,810,563 (1989).
[14] J.R. Hanrahan, Thermally Conductive Polytetrafluoroethylene Article, US Patent 5,738,936 (1998).
[15] A.L. Peterson, Thermally Conductive Organosiloxane Compositions, US Patent 5,011,870 (1991).
[16] M.J. Streusand, J.C. Getson, R.C. McAfee, Silicone Elastomers Having Thermally Conductive Properties, US Patent 4,544,696 (1985).
[17] G.A. Lane, Solar Heat Storage: Latent Heat Material, Vol. I, CRC Press, Boca Raton, FL, 1983.
[18] F.J. Whitfield, A.T. Doyel, Methods and Means for Conducting Heat from Electronic Components and the Like, US Patent 4,466,483 (1984).
[19] I.O. Salyer, Polyethylene Composites Containing a Phase Change Material Having a C14 Straight Chain, US Patent 4,711,813 (1987).
[20] I.O. Salyer, Phase Change Compositions, US Patent 4,797,160 (1989).
[21] J.C.H. Chen, J.L. Eichelberger, Encapsulated Phase Change Thermal Energy-storage Materials, US Patent 4,504,402 (1985).
[22] G.A. Lane, H.E. Rossow, Reversible Liquid/Solid Phase Change Composition for Storing Energy, US Patent 4,637,888 (1987).
[23] A. Kurklu, Renewable Energy 13 (1998) 89.
[24] M. Marinkovic, R. Nikolic, J. Savovic, S. Gadzuric, I. Zsigrai, Solar Energy Mater. Solar Cells 51 (1998) 401.
[25] H. Bo, E.M. Gustafsson, F. Setterwall, Energy 24 (1999) 1015.
[26] S.D. Sharma, D. Buddhi, R.L. Sawhney, Solar Energy 66 (1999) 483.
[27] J.F. Wang, G.M. Chen, F. Zheng, Int. J. Energy Res. 23 (1999) 277.
[28] A. Abhat, Solar Energy 30 (1983) 313.
[29] G. Egloff, Physical Constants of Hydrocarbons, Vol. 1, Reinhold, New York, 1939.
[30] S. Himran, A. Suwon, G.A. Manosoori, Energy Sources 16 (1994) 117.
[31] D. Pal, Y.K. Joshi, in: D. Agonater, M. Saka, Y.-C. Lee (Eds.), Advances in Electronic Packaging, Vol. 2, The American Society of Mechanical Engineers, New York, 1999, p. 1625.
[32] R. Clarksean, Y. Chen, M. Marongiu, in: D. Agonater, M. Saka, Y.-C. Lee (Eds.), Advances in Electronic Packaging, Vol. 2, The American Society of Mechanical Engineers, New York, 1999, p. 1611.
[33] R. Clarksean, Y. Chen, in: D. Agonater, M. Saka, Y.-C. Lee (Eds.), Advances in Electronic Packaging, Vol. 2, The American Society of Mechanical Engineers, New York, 1999, p. 1631.
[34] M. Telks, Ind. Eng. Chem. 44 (1952) 1308.
[35] G.A. Lane, H.E. Rossow, US Patent 4,272,390 (1981).
[36] N. Nishizaki, K. Sakagami, H. Okazaki, A. Mitsuibara, Japanese Patent Kokai 182 (1980) 55–82.
[37] K. Narita, H. Kimura, H. Ohama, K. Mutoh, J. Kai, Japanese Patent Kokai 585 (1975) 50–90.
[38] H. Miyoshi, K. Tanaka, Japanese Patent Kokai 990 (1978) 53–70.
[39] J.W. Dodd, H.T. Kenneth, Thermal Methods, Wiley, New York, 1987.
[40] T.F. Cheng, Comput. Mech. 23 (1999) 440.